Molecular Cancer Therapeutics

Spliceosome-Mediated RNA *Trans*-Splicing Facilitates Targeted Delivery of Suicide Genes to Cancer Cells

Christina Gruber[1], Iris K. Gratz[1], Eva M. Murauer[1], Elisabeth Mayr[1], Ulrich Koller[1], Leena Bruckner-Tuderman[2], Guerrino Meneguzzi[3,4], Helmut Hintner[1], and Johann W. Bauer[1]

Abstract

Patients suffering from recessive dystrophic epidermolysis bullosa (RDEB), a hereditary blistering disease of epithelia, show susceptibility to develop highly aggressive squamous cell carcinoma (SCC). Tumors metastasize early and are associated with mortality in the 30th–40th years of life in this patient group. So far, no adequate therapy is available for RDEB SCC. An approach is suicide gene therapy, in which a cell death-inducing agent is introduced to cancer cells. However, lack of specificity has constrained clinical application of this modality. Therefore, we used spliceosome-mediated RNA *trans*-splicing technology, capable of replacing a tumor-specific transcript with one encoding a cell death-inducing peptide/toxin, to provide tumor-restricted expression. We designed 3′ pre–*trans*-splicing molecules (PTM) and evaluated their efficiency to *trans*-splice an RDEB SCC-associated target gene, the matrix metalloproteinase-9 (*MMP9*), in a fluorescence-based test system. A highly efficient PTM was further adapted to insert the toxin streptolysin O (SLO) of *Streptococcus pyogenes* into the *MMP9* gene. Transfection of RDEB SCC cells with the SLO-PTM resulted in cell death and induction of toxin function restricted to RDEB SCC cells. Thus, RNA *trans*-splicing is a suicide gene therapy approach with increased specificity to treat highly malignant SCC tumors. *Mol Cancer Ther; 10(2); 233–41. ©2011 AACR.*

Introduction

Epidermolysis bullosa (EB) is a group of genetically and clinically heterogeneous diseases that are characterized by the formation of blisters and erosions on skin and mucous membranes following minor trauma (1). Patients suffering from recessive dystrophic EB (RDEB) harbour mutations in the *COL7A1* gene that cause decay of the respective mRNA. RDEB patients have a high risk of developing aggressive squamous cell carcinoma (SCC) in early adulthood. To date, neither chemo- nor radiotherapies yield satisfactory results, and despite extensive surgical excision of the tumor and surrounding tissue, recurrence and subsequent metastases are common. This explains the high mortality rate among patients with severe RDEB, who have a 70% cumulative risk of dying from metastatic SCC by the age of 45 years (2). Therefore, it is essential to develop effective molecular-based therapies for this cancer.

RNA *trans*-splicing allows an endogenous RNA to be converted into a new gene product via exon replacement. This can be achieved by the introduction of a designed pre–*trans*-splicing molecule (PTM) that binds to an endogenous target RNA and induces a *trans*-splicing reaction between the target and the PTM mediated by the spliceosome. PTMs contain a binding domain (BD), which defines the target specificity, splicing elements for efficient *trans*-splicing, and a coding sequence that is desired to replace a part of the target pre-mRNA (3). In this manner, *trans*-splicing has already been successfully used to repair the mutated part of disease-causing genes, indicating its potential use in gene therapy for several genetic disorders *in vitro* and *in vivo* (4–7).

The ability of *trans*-splicing technology to reprogram a pre-mRNA of interest offers numerous other applications, including suicide gene therapy for cancer treatment (8). Cancer suicide gene therapy entails delivery of various cytotoxic genes such as apoptotic factors or enzyme–prodrug combinations to cancer cells, leading to cell-specific expression and cell death. Suicide gene therapy has received much attention as a potent alternative to conventional anti-cancer therapies (9–11). In this context,

Authors' Affiliations: [1]Division of Molecular Dermatology and EB House Austria, Department of Dermatology, Paracelsus Medical University, Salzburg, Austria; [2]Department of Dermatology, University Medical Center Freiburg, Freiburg, Germany; [3]INSERM, U634, Nice, France; and [4]Université de Nice Sophia Antipolis, Faculté de Médecine, Nice, France

Note: Supplementary material for this article is available at Molecular Cancer Therapeutics Online (http://mct.aacrjournals.org/).

Current address for I.K. Gratz: Department of Pathology, University of California, San Francisco.

Corresponding Author: Christina Gruber, Division of Molecular Dermatology and EB House Austria, Department of Dermatology, Paracelsus Medical University, Salzburg, Muellner Hauptstrasse 48, 5020 Salzburg, Austria. Phone: 0043/662 4482-3118; Fax: 0043/662 4482-3125; E-mail: c.gruber@salk.at

doi: 10.1158/1535-7163.MCT-10-0669

Puttaraju and colleagues (12) successfully applied this method of *trans*-splicing to the tumor marker β-subunit of human chorionic gonadotropin gene 6 (β*hCG6*), which is expressed in many types of tumors but not, with a few exceptions, in normal adult cells. For this approach, intron 1 of β*hCG6* was targeted using a 3′ PTM encoding diphtheria toxin subunit A (DT-A), and correct *trans*-splicing was observed *in vitro* in cultured human lung cancer cells, as well as in an animal *in vivo* tumor model. Moreover, specific expression of the toxin was shown in tumor cells (12).

Trans-splicing technology offers significant advantages in suicide gene therapy when compared with conventional cDNA approaches. First, cancer cells can be specifically targeted by *trans*-splicing of an exclusive tumor marker gene within the cell. Therefore, this system provides increased safety through the specific expression of the cytotoxic protein in tumor cells, leaving normal, healthy cells surrounding the tumor intact. Second, the expression of the endogenous tumor marker mRNA is reduced due to its reprogramming by the *trans*-splicing reaction. Factors that promote tumor growth or invasion can be targeted by specific PTMs that reduce the endogenous levels of target RNA, resulting in a reduction of the target molecule's tumor-promoting effect.

Based on these facts we designed a PTM targeting the marker gene, matrix metalloproteinase-9 (*MMP9*), which is highly expressed in cultured RDEB SCC cells. Because little is known about the properties of BDs that promote the most effective *trans*-splicing reactions, we used a fluorescence-based test system to identify optimal PTMs (i.e., BDs). The selected PTM was further investigated for its ability to induce specific cell death by reprogramming *MMP9* through a *trans*-splicing reaction to express the toxin streptolysin O (SLO) of *Streptococcus pyogenes*.

Materials and Methods

Plasmids

Target molecule. In the fluorescence screening procedure used to identify potent PTMs for the *trans*-splicing reaction, we designed a target molecule containing the 5′ half of green fluorescent protein (GFP) coding sequence and intron 1/exon 2 of the *MMP9* gene. The 5′ half of GFP (336 bp) was amplified from pIRES-AcGFP1 (Clontech) using Pfu Turbo DNA polymerase (Stratagene). The reverse primer inserted an EcoRV restriction site and a 5′ splice site (ss; aggta) at the GFP/intron border, the latter of which is indispensable for the *trans*-splicing reaction (5′GFP forward 5′caccatggtgagcaaggg3′, reverse 5′gatatctcttacctcggcgcgactt3′). The 5′ part of GFP was then subcloned into the TOPO cloning sites of pcDNA3.1D/V5-His-TOPO (Invitrogen) according to the manufacturer's instructions. Primers amplifying intron 1 and exon 2 of *MMP9* from human genomic DNA were designed to include EcoRV and NotI restriction sites (forward 5′gagagatatcgtgggcaaacacctagtct3′, reverse 5′gagagcggccgccaataggtgatgttgtggtgg3′) and the PCR product was finally cloned into pcDNA3.1D.

PTM screening molecule. The PTM molecule is based on pcDNA3.1D/V5-His-TOPO harboring the 3′ part of GFP as well as splicing elements [spacer, branch point, and polypyrimidine tract (PPT)] previously described by Dallinger et al. (13). The 470-bp fragment of 3′ GFP was amplified using a forward primer carrying an *Eco*RI site, which also served as the restriction site for ligation of variable BDs.

BDs complementary to intron 1 of *MMP9* were amplified from human genomic DNA to yield 150-bp BD2 and BD4 (BD2, forward 5′gagagaattcgtgggcaaacacctagtct3′ and reverse 5′tctctcgaattctgcctaaccctggacac3′; BD4, forward 5′gagagaattcatgcagctgtggggtagaa3′ and reverse 5′tctcgaattcatgcccagcagggacta3′). Oligonucleotides encoding the shorter BD1 (45 bp) were synthesized with *Eco*RI restriction sites (Eurofins MWG Operon), annealed, and subcloned into PTM vector.

To determine the transfection efficiency of the PTM, sequences encoding an internal ribosomal entry site (IRES) as well as the reporter gene DsRed were inserted into the vector. The wild type IRES sequence was amplified from pIRES2-AcGFP1 and ligated between *Eco*RV and *Xma*I restriction sites. The full-length DsRed gene was cut out of pDsRed Monomer (Clontech) using *Eco*RV and *Not*I restriction enzymes and cloned into the PTM vector between those two restriction sites.

The control vector for FACS analysis consisted of a full-length GFP gene, an IRES sequence, and a full-length DsRed gene.

PTM-S1. The *MMP9* suicide PTM-S1 was designed in the vector pIRES-AcGFP1, containing 3′ splice elements identical to those of the PTM molecule used in the screening procedure. In addition, a glycine–alanine linker was inserted after the ss of the PTM to guarantee accurate expression and folding of the fusion protein after specific *trans*-splicing. Therefore, oligos were designed with a *Pst*I site at the 5′ end (5′gggcgccggagccggatcaggcgcaggagccggcgcca3′) and an *Spe*I site on the 3′ end (5′ctagtggcgccggctcctgcgcctgatccggctccggcgccctgca3′) of the linker. In addition, GFP was excised and the coding sequence of truncated SLO (tSLO) or thymidine kinase (*tk*) of herpes simplex virus was inserted into the plasmid after the linker sequence. The resulting PTM tSLO cassette was further cloned into a modified SV40 vector, which harbors fewer 3′ ss motifs, thus reducing unwanted *cis*-splicing events within the plasmid. A vector expressing the fusion protein of *MMP9* exon 1 and tSLO served as a positive control for the suicide assays, because this fusion protein is also expressed by the cancer cells upon correct *trans*-splicing between the suicide PTM and the target gene *MMP9*. Furthermore, the resulting fusion protein should be secreted due to an endoplasmic reticulum (ER) signal present in exon 1 of *MMP9*. The correct recognition of this ER signal and cleavage site was predicted by using SignalP 3.0 software (http://www.cbs.dtu.dk/services/SignalP/).

Tissue samples and cell lines

Tissue samples were taken in the course of a surgery at the Department of Children's Surgery, University Hospital Graz, Austria, and used with informed consent. Biopsies of both SCC and nonaffected skin were taken from the same RDEB patient (*COL7A1*, 4048–1G>T/8440 C>T). The RDEB keratinocyte cell line (*COL7A1*, 3760–1G>A/unknown), E6/E7 immortalized, was kindly provided by Prof. G. Meneguzzi, Nice, France, in 2007 and the spontaneously immortalized RDEB SCC cell line (SCC–EB–GER, MN270503, *COL7A1*, 8244insC/8244insC) was obtained from Prof. L. Bruckner-Tuderman, Freiburg, Germany, in 2007. All cells were routinely grown in keratinocyte–serum-free medium (Gibco Invitrogen) at 37°C in 5% CO_2.

In addition, human embryonic kidney cell line, HEK293AD (Stratagene, 2007), was used for the PTM screening experiments and grown in DMEM, 10% FCS and Pen/Strep. The cell line was authenticated by the company. All experiments were done under endotoxin-free conditions.

Each initial RDEB/RDEB SCC cell line stock and random passages were verified by detecting the specific *COL7A1* mutation performing direct sequencing of genomic DNA. Mycoplasma infection was ruled out by PCR analysis, as previously reported (14), in each cell line prior to experimental use.

Semi-quantitative real-time PCR and reverse transcriptase PCR

Total RNA was isolated from RDEB SCC tissue samples using RNeasy Lipid Tissue Mini Kit (Qiagen) according to the manufacturer's instructions. A Bio-Rad iCycler system (BioRad) was used to assess transcript levels of *MMP* genes in tissue samples as well as in cell lines. All primer pairs were designed using Primer3 Software (http://frodo.wi.mit.edu/cgi-bin/primer3/primer3_www.cgi). The integrity of PCR products was analyzed by agarose gel and sequence analysis. All PCRs were carried out in duplicate, and the mean and standard deviation were calculated from 3 independently done experiments. Transcript levels in the various samples were calculated after normalization to the housekeeping gene for α-tubulin.

Reverse transcriptase PCR (RT PCR; SuperScript One-Step RT-PCR, Invitrogen) was used for detection of endogenous *trans*-splicing between the target gene *MMP9* and PTM-BD1 containing *tk*. RNA was isolated 48 hours after PTM transfection and PCR was done using forward primer 5′gtcctggtgctcctggtg3′ and reverse primer 5′agatgttcgcgattgtctcggaa 3′. In addition, a nested PCR was carried out using forward primer 5′ttccctggagacctgagaac3′ and reverse primer 5′gtaagtcatcggctcgggta3′ to verify the correct PCR products.

Western blot analysis

For immunoblot analysis, cells were cultured until confluency and resuspended with lysis buffer (0.5 mol/L Tris-HCL, pH 6.8, 20% glycine, 10% SDS, and 5% β-mercaptoethanol) in the presence of protease inhibitor (Complete Mini protease inhibitor cocktail tablets, Roche). Proteins from tissue samples were extracted using TRI Reagent (Sigma-Aldrich) according to the manufacturer's protocol. Samples were resolved on a denaturating 10% SDS-polyacrylamide gel and transferred to a nitrocellulose membrane (Hybond-TM-ECLTM, Amersham Biosciences) by electroblotting according to standard techniques. The membrane was blocked with 1% blocking buffer (Roche) during 1 hour at room temperature and incubated overnight at 4°C with anti–MMP-9 pAB (Abcam). A polyclonal antibody against tubulin beta (Abcam) served as loading control. HRP labeled EnVision+ anti-rabbit antibody (Dako) was used as secondary antibody. Bands were visualized using Immun-Star WesternC Chemiluminescent Kit (BioRad) and ChemiDoc XRS Imager (BioRad).

Streptolysin O

Streptococcus pyogenes was obtained from patient throat swabs and routinely grown on blood agar plates (Sigma-Aldrich). PCR amplification of a truncated version of SLO from *S. pyogenes* was done by adapting the protocol of Yang et al (15). A smear of *S. pyogenes* was pretreated by incubation at 95°C for 30 minutes and the lysate was used for PCR with GoTaq hot start polymerase (Promega), 2 mmol/L dNTPs, and forward and reverse primer pairs (150 μmol/L), the latter primer harboring a *BamH*I restriction site for subcloning into PTM-S1 vector. SLO forward primer (5′ttcgaacaaacaaaacactgc3′) and reverse primer (5′gttcgattacttataagtagggatccgagaga3′) were used to amplify a 32-amino acid truncated version of SLO, named tSLO. Sequence analysis revealed that the amplified tSLO DNA differed from a previously reported sequence (GenBank accession number AB050250) at 6 amino acid positions: Ser47→Asn47; Arg172→Met172; Asn182→Asp182; Asp324→Glu324; Gln470→Arg470; Trp535→Arg535. In addition, the cell-killing activity of tSLO was confirmed by lactate dehydrogenase (LDH) release assay.

PTM screen

One microgram of the the target molecule and 3 μg of the PTM vector, harboring a single BD, were transiently transfected into HEK 293AD cells using EcoTransfect (OZ Biosciences). A total of 10^6 cells were used for transfections according to the manufacturer's protocol. Analyses using a fluorescence microscope (epifluorescence Zeiss Axioskop) and a FACS instrument (Beckmann Coulter FC500) were done 48 hours post-transfection. For fluorescence analysis, cells were washed and resuspended in 1 mL FACS buffer (Dulbeco's PBS, 3% fetal calf serum) and kept on ice. Thirty thousand events were recorded and data were analyzed using CXP software (Beckmann Coulter).

Cytotoxicity studies

Recessive dystrophic epidermolysis bullosa SCC cells were transiently transfected with PTM-S1 and control

vectors using the AMAXA system (Lonza), which gives a transfection efficiency of about 40%. Cells were harvested after 24 hours under standard conditions. Permeable cells were further stained with 7-aminoactinomycin D (7-AAD) and analyzed by FACS. LDH release by membrane-permeabilized cells was monitored using a *CytoTox 96* nonradioactive cytotoxicity assay (Promega) following the manufacturer's instructions.

Cytotoxicity upon functional *trans*-splicing of the PTM in RDEB as well as RDEB SCC cells was assessed by an 3 (4,5 dimethylthiazol-2-yl) 2,5 diphenyltetrazolium bromide (MTT) assay. Cells were transfected with the PTM-S1 or control vectors and seeded into 96-well plates. Twenty-four hours after transfection, MTT (5 g/L) was added to each well and incubated for 1 hour at 37°C. Finally, cells were lysed with glycine/dimethyl sulfoxide and absorbance of the resultant formazan product was measured at 492 nm with a photometer (Tecan).

Results

Identification of *MMP9* as a target gene in an RDEB SCC cell line for suicide *trans*-splicing

To identify a target gene upregulated in RDEB SCC, we did semi-quantitative real-time PCR analysis using RNA isolated from RDEB SCC, as well as peritumoral tissue samples from the same EB patient. Moreover, expression levels were also analyzed in cell lines (RDEB SCC and RDEB cell lines) which were used in further *in vitro* studies. Due to the fact that RDEB SCC is characterized by rapid tumor growth and invasion of the extracellular matrix, we focused on the mRNA expression levels of several matrix MMPs (*MMP3*, *MMP7*, *MMP9*, and *MMP13*), which had already been described as differentially regulated proteins in EB-associated cancer (16).

Semi-quantitative real-time PCR analysis revealed increased expression of the *MMP3*, *MMP9*, and *MMP13* genes in tumor tissue compared with peritumoral skin, whereas *MMP7* was found to be downregulated (Fig. 1A). In contrast to tumor tissue, we could hardly detect any *MMP3* and *MMP7* mRNA expression in cultured RDEB SCC cells. *MMP9* and *MMP13* showed increased mRNA levels when normalized to the RDEB cell line (Fig. 1B). Moreover, MMP-9 protein expression was further confirmed by Western blot analysis showing an elevated level in RDEB SCC cells compared with RDEB cells (Fig. 1C). Because the amount of *MMP9* mRNA was elevated compared with that of *MMP13* and the difference between RDEB and RDEB SCC cells showed higher statistical significance, we chose to use the *MMP9* gene to provide the proof of principle for *trans*-splicing technology in a suicide gene therapy approach for RDEB SCC *in vitro*.

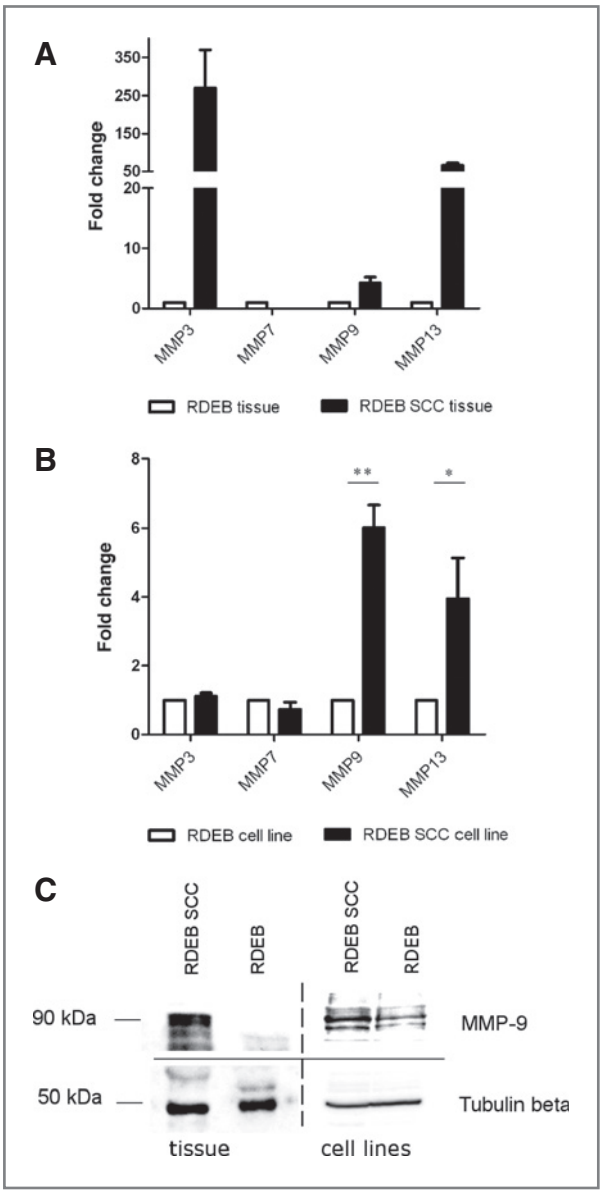

Figure 1. *MMP9* is overexpressed in an RDEB SCC cell line. Real-time PCR analysis was done to detect the expression of various MMPs in a RDEB tumor tissue sample (A) as well as a cell line (B). The mRNA levels were calculated relative to the housekeeping gene α-tubulin and normalized to peritumoral RDEB tissue or cell line. Data are presented as the mean of 3 independent experiments ± SD. Significance was determined using Student's *t* test, $P < 0.05$ (*), $P < 0.005$ (**). C, Western blot analysis with extracts from tissues and cell lines of RDEB SCC and RDEB using an anti–MMP-9 antibody. Tubulin beta protein levels served as control for quantity and quality.

PTM selection using a fluorescence-based testing system

A PTM can theoretically target any intronic region of a given RNA through its complementary BD that brings specificity to the *trans*-splicing reaction. However, sequence, length, and steric constraints of the BD can affect its efficiency and specificity in the reaction. To identify a PTM harboring a BD with optimized characteristics for *trans*-splicing into intron 1 of the target gene *MMP9*, we established a fluorescence-based testing system (Fig. 2) as described by Mitchell and McGarrity (17).

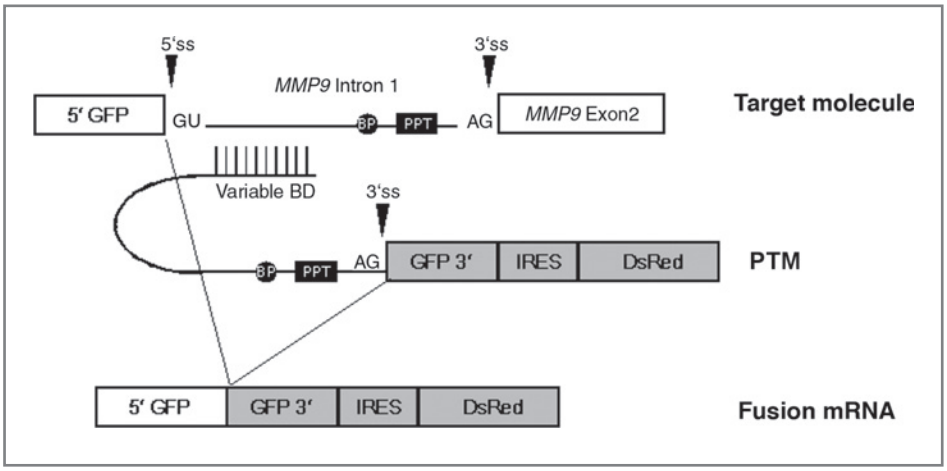

Figure 2. Schematic diagram of the fluorescence *trans*-splicing test system. The PTM binds specifically through an antisense BD to *MMP9* intron 1 provided by the target molecule. Correct *trans*-splicing between the 5′ splice site of the target molecule and the 3′ splice site of the PTM results in a reprogrammed mRNA encoding full-length GFP protein as well as a DsRed reporter molecule. BP, branch point; PPT, polypyrimidine tract.

In this experimental setup, the fluorescent protein GFP is expressed only upon accurate *trans*-splicing, which fuses 2 halves of the GFP mRNA to make a full-length mRNA. We constructed a target vector harboring the 5′ half of GFP and sequence of *MMP9* intron 1/exon 2. Each tested PTM comprises a BD complementary to different parts of the sequence of *MMP9* intron 1, a 3′ splicing domain including a branch point, a PPT and a 3′ ss, as well as the 3′ half of GFP. Downstream of the 3′ half of GFP, we inserted an IRES and the reporter molecule DsRed to monitor transfection efficiency. Precise *trans*-splicing between the target molecule and the PTM in cotransfected cells leads to a complete and functional GFP, which can be examined directly by fluorescence microscopy or FACS analysis.

To select a BD that promotes *trans*-splicing most efficiently, we designed 3 different PTMs, each consisting of a randomly chosen antisense BD (BD1, BD2, and BD4) for *MMP9* intron 1 (Supplemement 1).

The target molecule and each PTM were cotransfected in HEK293 cells and the expression of full-length GFP, indicating correct *trans*-splicing, was monitored by fluorescence microscopy (Fig. 3A). No GFP signal was detected in cells transfected with either target molecule or PTM alone (data not shown). A plasmid simultaneously expressing DsRed and GFP served as a positive control. In this setup, we observed differences in *trans*-splicing reactions between the target molecule and the PTM harboring different BDs. The PTM containing BD1 produced strong GFP expression, indicating efficient *trans*-splicing, whereas PTM BD2 induced only weak green fluorescence signal, indicating low *trans*-splicing efficiency. Finally, PTM BD4 did not seem to induce *trans*-splicing at all, as the BD4 transfectants produced virtually no GFP expression.

To quantify the *trans*-splicing events we did FACS analysis using HEK293AD cells cotransfected with the target molecule and a PTM (Fig. 3B). The data are displayed as the ratio of DsRed fluorescence (PTM transfection) against the level of GFP expression and thus, the *trans*-splicing events (Fig. 3C). The *trans*-splicing performance varied between different PTMs (BD1>BD2>BD4), demonstrating the significance of both the binding site and the sequence of the BD. The results of the FACS analysis correspond with the images obtained by fluorescence microscopy. In this screening procedure, BD1 was identified as the most efficient BD and was therefore used for further *in vitro* studies.

Trans-splicing in RDEB cancer cells

Next, we sought to show *trans*-splicing between the PTM and the endogenous target mRNA *in vitro* at the mRNA level. Therefore, the RDEB SCC cell line was transfected with a vector expressing PTM-BD1 and a cDNA of *tk* from herpes simplex virus. In the presence of the antiviral drug ganciclovir, *tk* produces toxic metabolites that disrupt DNA synthesis and result in the death of dividing cells. Forty-eight hours after transfection and without addition of ganciclovir, correct *trans*-splicing was confirmed by RT PCR using primers with specific binding sites within exon 1 of *MMP9* and *tk* (Fig. 4A). The PCR product was further verified by direct sequencing, confirming successful PTM-driven *trans*-splicing of the target gene *MMP9* (Fig. 4B and C). With this experimental approach, we were able to show *trans*-splicing between endogenous *MMP9* and PTM-BD1 at the mRNA level, proving the functionality of our designed PTM.

PTM containing the toxin SLO is functional in a cell culture model

For endogenous suicide studies, we designed a new PTM, designated as PTM-S1, containing the binding domain BD1 (Supplement 2) and a truncated version (del32aa) of the cell death-inducing peptide SLO (15,18), designated as tSLO. tSLO was inserted into PTM-S1 with the goal to induce specific cell death in *MMP9*-overexpressing tumor cells. In our experimental approach, the toxin is expressed as a fusion protein with *MMP9* exon 1 upon correct *trans*-splicing. Because both the *MMP9* gene and SLO contains an ER-targeting signal,

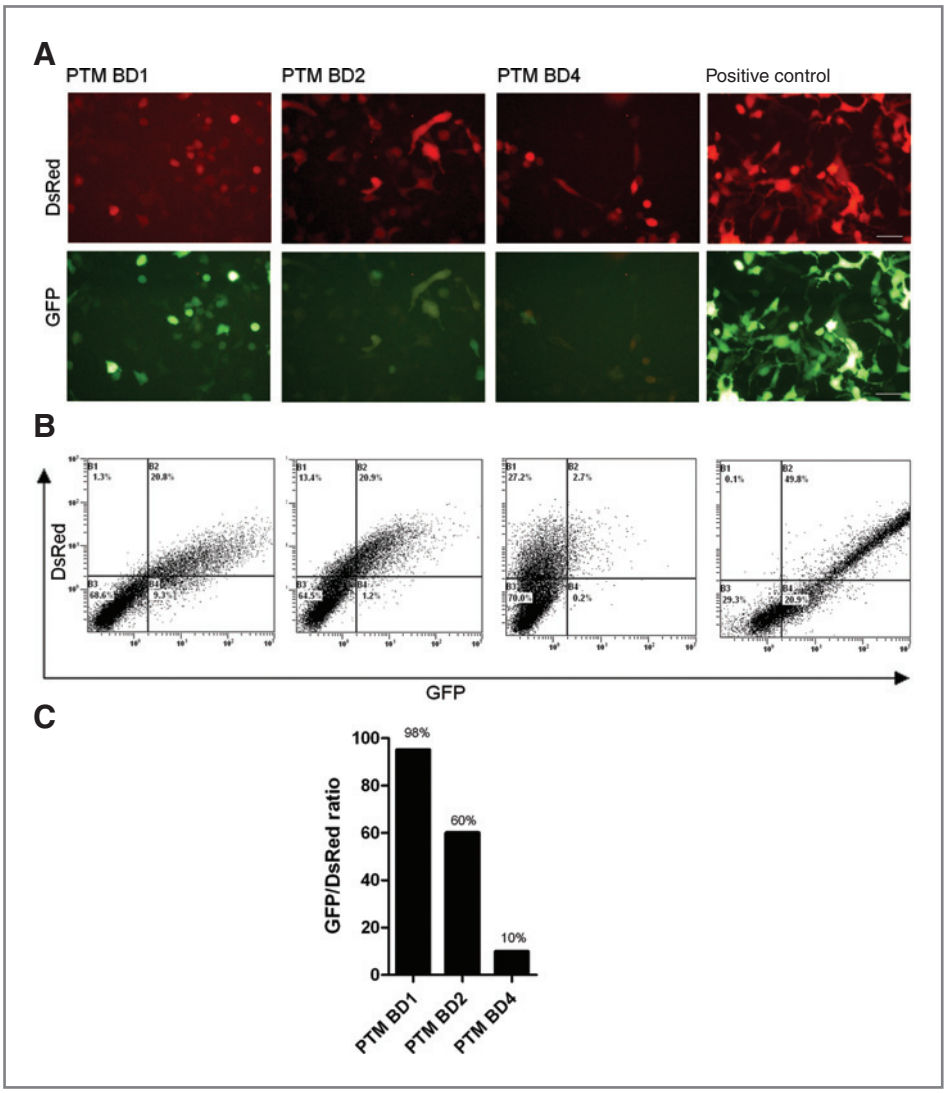

Figure 3. Fluorescence microscopy and FACS analysis of double-transfected HEK293AD cells. A, visualizing *trans*-splicing in double-transfected HEK293AD cells by fluorescence microscopy. Positive control is a construct that contains DsRed as well as a full-length GFP cDNA and therefore shows protein expression of both molecules. In double-transfected cells the detection of DsRed expression only provides information on the efficiency of plasmid transfection. GFP-expressing cells indicate accurate *trans*-splicing of the target gene and the PTM harboring one of 3 different BDs (BD1, BD2, and BD4). B, DsRed$^+$ cells result from efficient PTM transfection of cells, whereas DsRed$^+$GFP$^+$ double-positive cells result from successful *trans*-splicing. The positive control shows GFP and DsRed expression in equal amounts. GFP single-positive cells reflect the brighter fluorescence typically obtained with GFP over DsRed. C, diagram representing the GFP/DsRed ratio of each PTM (PTM BD1, PTM BD2, or PTM BD4) in double-transfected cells. GFP/DsRed ratio efficiency was calculated by the amount of total GFP$^+$ (GFP$^+$ and GFP$^+$DsRed$^+$) cells with respect to all PTM-transfected cells (total DsRed$^+$). Scale bars: 20 μm.

we used a truncated version of SLO lacking the ER-targeting signal to guarantee correct processing and avoid secretion of SLO without *trans*-splicing with *MMP9*. In addition the del32aa version has been used successfully in a suicide gene therapy approach *in vivo* and *in vitro* in a study by Yang et al (15). The resulting fusion protein upon correct *trans*-splicing was predicted to be secreted by the transfected tumor cells and this enables the toxin to attack the tumor cell also from the outside, suggesting higher efficiency in RDEB SCC cells.

To monitor specific cell death upon PTM-S1 treatment, we did 2 independent cell culture assays. First, the amount of dead cells after transfection of RDEB SCC cells with PTM-S1 containing tSLO was monitored in a 7-AAD uptake experiment (Fig. 5A).

Cells transfected with the suicide PTM-S1 showed high levels of 7-AAD cell staining. Twenty-four hours after transfection, 22.9% of the PTM-transfected SCC cell population was dead, as shown by 7-AAD positive staining. This indicated expression of the MMP-9 exon 1/tSLO fusion protein upon *trans*-splicing (Fig. 5A). We also detected cytotoxicity (18%) in cells transfected with a control plasmid (mock, backbone of PTM), which resulted from the transfection procedure itself. Similar levels of cytotoxicity were observed between PTM-S1 and the positive control (24%) encoding the fusion protein MMP-9/tSLO. In a second approach, we wanted to investigate whether the cytotoxicity of PTM-S1 was caused by cell membrane permeabilization resulting from SLO expression. We measured the release of cytosolic LDH, an assay specifically used for the measurement of cell lysis by perforins or other pore-forming toxins. As shown in Figure 5B, PTM-S1 treatment of RDEB cancer cells resulted in increased LDH concentration detected in the supernatant, indicating that correct *trans*-splicing led to expression of MMP-9/tSLO fusion protein.

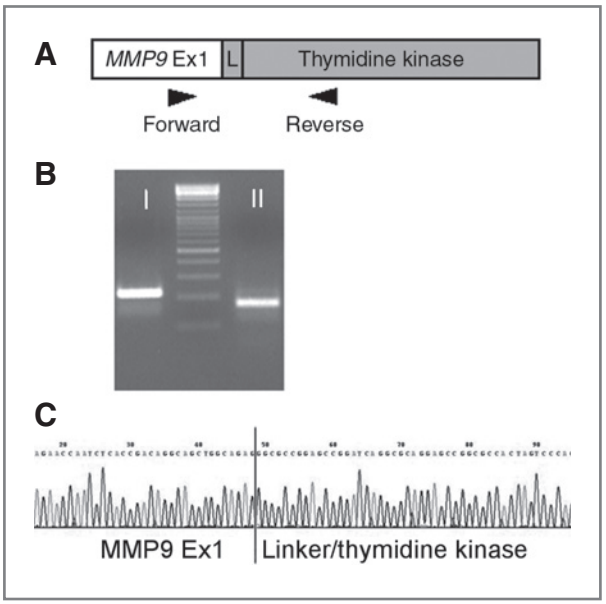

Figure 4. Correct *trans*-splicing to endogenous *MMP9* mRNA. A, primer pair used in nested PCR analysis for detection of *MMP9/tk* fusion mRNA. Primer locations are marked by arrowheads. B, specific *trans*-splicing was shown in PTM-transfected RDEB SCC cells by the presence of a 210-bp PCR product, which is shown on the agarose gel (I) in contrast to untransfected cells (II). C, further sequence analysis revealed that *tk* was successfully *trans*-spliced to the target gene *MMP9*. The PCR band shown in lane II was also analyzed by direct sequencing and proven to be a nonspecific PCR product.

Selective cytotoxicity by specific PTM-S1 in *MMP9*-expressing cancer cells

We further determined whether the PTM-induced toxin expression is selective for *MMP9*-expressing cancer cells. Therefore, we transiently transfected the vector encoding PTM-S1 into RDEB SCC cells expressing high *MMP9* levels, as well as RDEB cells that express low levels of *MMP9* mRNA to assess the target specificity of PTM-S1. The MTT assay showed significant cytotoxicity in both cell lines when transfected with the positive control construct that encodes the fusion protein MMP-9/tSLO not requiring *trans*-splicing (Fig. 6). However, only RDEB SCC cells, but not RDEB keratinocytes, showed a significant reduction in cell viability ($P < 0.005$) upon transfection with PTM-S1. These data indicate the requirement of *MMP9* marker gene expression for specific *trans*-splicing, providing valuable target-cell specificity.

Discussion

Squamous cell carcinomas that arise in patients with RDEB are very aggressive and metastasize early. To date, no successful treatment has been achieved by conventional approaches (2). In this study, we report the development of a suicide gene therapy approach that selectively kills RDEB cancer cells through RNA *trans*-splicing.

In the first series of experiments, we identified *MMP9* as being upregulated in both SCC tissues from an RDEB patient and an RDEB SCC cell line compared with non-SCC RDEB skin tissue and an RDEB cell line. MMP-9 is a zinc metalloendopeptidase that degrades and removes extracellular matrix molecules from tissues and is involved in tissue remodeling, wound healing, and cancer invasiveness (19). Although previous immunohistological studies of several MMPs in RDEB SCC tissue reported that MMP-9 expression is restricted to inflammatory cells (16), we showed here that RDEB SCC cells in culture also express *MMP9* at the mRNA level as well as the protein level. Based on these data, we evaluated a PTM designed to replace the target gene *MMP9* with the toxin SLO through a *trans*-splicing reaction. We have shown that PTM-S1 induces correct *trans*-splicing to the endogenous *MMP9* mRNA, leading to expression of functional SLO and thus cancer cell death. Notably, the PTM caused cytotoxicity in MMP9-positive cancer cells, indicating target-specific RNA replacement.

The BD of a PTM molecule is the most critical element for accurate *trans*-splicing. It ensures specificity for target–gene binding, which in turn defines the specificity of tumor cell targeting. This approach thus offers an important advantage compared with other conventional therapies. Most *trans*-splicing studies have been done with PTMs containing BDs in the range of 70–250 bases (6,20,21). It has been shown that enlargement of BD size improves *trans*-splicing efficiency (22). In previous studies, we observed that localization of the binding site within the target intron also influences the *trans*-splicing efficiency. Therefore, we analyzed the *trans*-splicing activity of 3 different BDs complementary to *MMP9* intron 1 using a fluorescence-based model system. Puttaraju et al. (12) showed improvement of PTMs by extension of BD length. Our data here show that not only the size but also the position of the binding site in the intron may contribute to stringent binding because the shorter BD1 (45 bp) showed superior *trans*-splicing activity. It is also likely that BD properties are difficult to generalize because the PTMs are designed for different intronic regions of various genes. Therefore, these data emphasize that screening experiments for the best BDs should be done with every new target gene that is selected to be used in *trans*-splicing suicide gene therapy.

The efficiency of RNA *trans*-splicing *in vitro* is an important question because the low transfection rates of tumor cells still constitute a limiting factor (23). Detection of endogenous *trans*-splicing efficiencies was done in gene correction studies (e.g., of factor VIII in hemophilia A), showing *trans*-splicing levels of 3%–7%, depending on the PTM construct (24,25). Therefore, *trans*-splicing seems to be a low-efficiency event; however, it is expected that in suicide gene therapy, this low *trans*-splicing efficiency can be at least partly offset by the high efficacy of most toxins, as only a few molecules are usually required for cell death induction, for example, a single molecule of DT-A can kill a target cell (26). Moreover, in conjunction

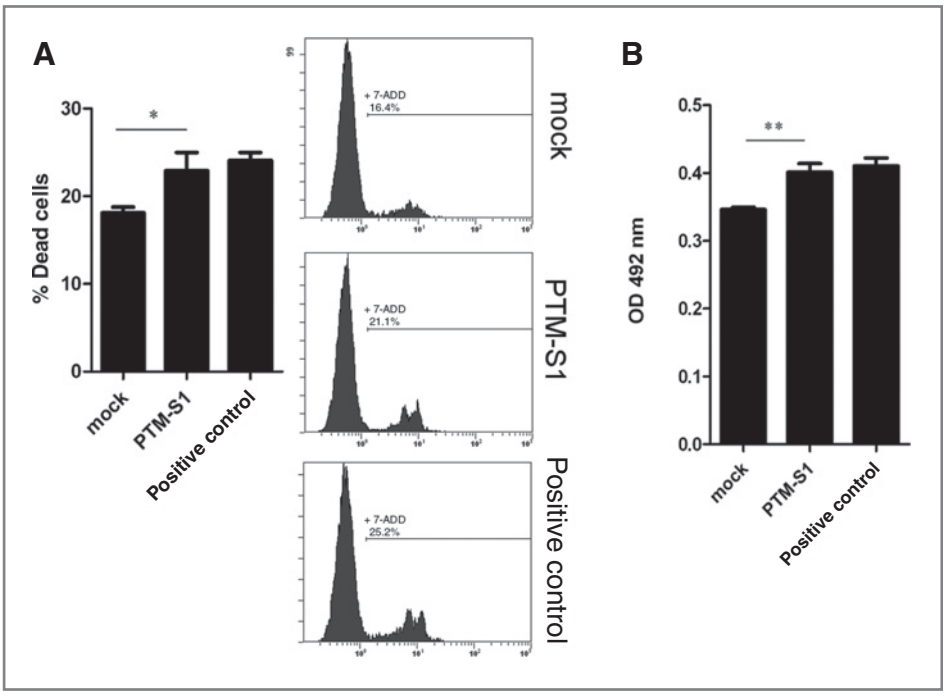

Figure 5. *Trans*-splicing of target gene induces tSLO expression and subsequent cell death. A, the uptake of 7-AAD by transfected RDEB SCC cells was monitored by FACS analysis 24 hour after transfection. The percentage of dead cells (+ 7-AAD) was calculated using CXP software (Beckman Coulter). The positive control encodes the fusion protein of MMP-9 exon 1 and tSLO, which will also be present after correct *trans*-splicing events. The cytotoxicity of the transfection method itself was investigated by transfection of the PTM backbone plasmid (mock). The experiment was repeated 4 times (mean ± SEM) and 1 representative histogram of 7-AAD stainings is shown. B, LDH release assay upon cell-membrane permeabilization caused by SLO. The release of cytosolic LDH into the culture medium was measured using a CytoTox 96 nonradioactive cytotoxicity assay kit. RDEB SCC cells were transfected with 1 μg of each construct and culture media was harvested for 24 hours. Data were generated by measurement of absorbance at 492 nm. One representative experiment in triplicate ± SD out of 3 is shown.

with suicide gene therapy *in vivo*, adjunct therapies to stimulate the immune system could also be employed to combat tumor formation in cancers such as SCC, which take measures to evade immune recognition (27,28).

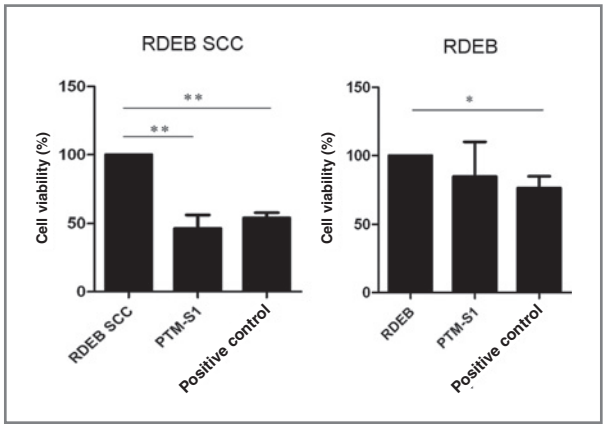

Figure 6. Specific induction of suicide gene activity by *MMP9*-specific *trans*-splicing PTM-S1 in RDEB SCC. Cell lines were transfected with PTM-S1 or the positive control and analyzed for cell-specific cytotoxicity after 24 hours using MTT assay. Cell viability is represented as a percentage relative to RDEB SCC or RDEB cells transfected with water. Data are shown as the mean of 3 independent experiments ± SD. Significance $P < 0.05$ (*), $P < 0.005$ (**).

Activation of the immune system can be achieved by boosting immune recognition and response using strong danger signals such as products of cell injury or necrotic cell death, as well as signals generated by inflammation (29). Therefore, SLO might be a suitable suicide gene for cancer gene therapy because it induces cell death by necrosis (15) and thus releases heat shock proteins (HSP). Because endogenous HSP70 is a natural ligand of mammalian Toll-like receptor 4, HSP70 may serve as an immune-activating danger signal in the tumor environment (30). This fact could further increase the efficacy of suicide gene therapy and may thus partly compensate for the lower transfection rates obtained with standard techniques.

Attention has also been drawn to the specificity of the PTM because nonspecific *trans*-splicing events have already been observed. For this reason, we tested the specificity of PTM-S1 toxicity toward *MMP9*-expressing cells. In cells that expressed low levels of *MMP9*, we observed some toxicity, although the levels were not significantly different from those of the nontransfected control cells. As the *MMP9* levels are low but not zero in the RDEB cell line, we expect that the observed low-level toxicity resulted from *MMP9*-specific *trans*-splicing rather than from nonspecific *trans*-splicing events.

In summary, the results presented here indicate that 3′ *trans*-splicing constitutes an alternative tool for suicide gene therapy. We showed that spliceosome-mediated RNA *trans*-splicing is able to target tumor cells by using specifically designed molecules (PTMs) that induce binding and *trans*-splicing of an endogenous tumor-associated marker gene. We also showed that targeted cell death in RDEB tumor cells can be achieved by a specifically designed PTM delivering the toxin SLO. Therefore, this work shows a promising application of *trans*-splicing technology to be used in further *in vivo* suicide gene therapy studies.

Disclosure of Potential Conflicts of Interest

J.W. Bauer has a patent pending on *trans*-splicing.

Acknowledgments

We thank Debra Europe/EB-SCC bank for providing the RDEB-SCC cell line and Markus Hell, M.D., (Department of Microbiology, Paracelsus University Hospital, Salzburg, Austria) for providing the bacterial culture of *Streptococcus pyogenes*.

Grant Support

This work was funded by DEBRA Austria.
The costs of publication of this article were defrayed in part by the payment of page charges. This article must therefore be hereby marked *advertisement* in accordance with 18 U.S.C. Section 1734 solely to indicate this fact.

Received July 14, 2010; revised October 25, 2010; accepted November 11, 2010; published OnlineFirst January 5, 2011.

References

1. Lanschuetzer CM, Fine JD. Classification and molecular basis of hereditary epidermolysis bullosa. In:Fine JD, Hintner H, editors. Life with Epidermolysis Bullosa (EB): Etiology, Diagnosis, Multidisciplinary Patient Care, and Therapy. NewYork: Wien Springer; 2008. p.6–24.
2. Fine JD, Johnson LB, Weiner M, Li KP, Suchindran C. Epidermolysis bullosa and the risk of life-threatening cancers: The National EB Registry experience, 1986–2006. J Am Acad Dermatol 2009;60: 203–11.
3. Mansfield SG, Chao H, Walsh CE. RNA repair using spliceosome-mediated RNA trans-splicing. Trends Mol Med 2004;10:263–8.
4. Chen HY, Kathirvel P, Yee WC, Lai PS. Correction of dystrophia myotonica type 1 pre-mRNA transcripts by artificial trans-splicing. Gene Ther 2009;16:211–7.
5. Murauer EM, Gache Y, Gratz IK, Klausegger A, Muss W, Gruber C, et al. Functional correction of type VII collagen expression in dystrophic epidermolysis bullosa. J Invest Dermatol 2011;131: 74–83.
6. Wally V, Klausegger A, Koller U, Lochmuller H, Krause S, Wiche G, et al. 5′ trans-splicing repair of the PLEC1 gene. J Invest Dermatol 2008;128:568–74.
7. Wang J, Mansfield SG, Cote CA, Du Jiang P, Weng K, Amar MJA, et al. Trans-splicing into highly abundant albumin transcripts for production of therapeutic proteins in vivo. Mol Ther 2009;17:343–51.
8. Garcia-Blanco MA, Puttaraju M, Mansfield SG, Mitchell LG. Spliceosome-mediated RNA trans-splicing in gene therapy and genomics. Gen Ther Reg 2000;1:141–63.
9. Gottesman MM. Cancer gene therapy: an awkward adolescence. Cancer Gene Ther 2003;10:501–8.
10. Natsume A, Yoshida J. Gene therapy for high-grade glioma: current approaches and future directions. Cell Adh Migr 2008;2:186–91.
11. Xu F, Li S, Li XL, Guo Y, Zou BY, Xu R, et al. Phase I and biodistribution study of recombinant adenovirus vector-mediated herpes simplex virus thymidine kinase gene and ganciclovir administration in patients with head and neck cancer and other malignant tumors. Cancer Gene Ther 2009;16:723–30.
12. Puttaraju M, Jamison SF, Mansfield SG, Garcia-Blanco MA, Mitchell LG. Spliceosome-mediated RNA trans-splicing as a tool for gene therapy. Nat Biotechnol 1999;17:246–52.
13. Dallinger G, Puttaraju M, Mitchell LG, Yancey KB, Yee C, Klausegger A, et al. Development of spliceosome-mediated RNA trans-splicing (SMaRT) for the correction of inherited skin diseases. Exp Dermatol 2003;12:37–46.
14. Uphoff CC, Drexler HG. Comparative PCR analysis for detection of mycoplasma infections in continuous cell lines. In Vitro Cell Dev Biol Anim 2002;38:79–85.
15. Yang WS, Park SO, Yoon AR, Yoo JY, Kim MK, Yun CO, et al. Suicide cancer gene therapy using pore-forming toxin, streptolysin O. Mol Cancer Ther 2006;5:1610–9.
16. Kivisaari AK, Kallajoki M, Mirtti T, McGrath JA, Bauer JW, Weber F, et al. Transformation-specific matrix metalloproteinases (MMP)-7 and MMP-13 are expressed by tumour cells in epidermolysis bullosa-associated squamous cell carcinomas. Br J Dermatol 2008;158:778–85.
17. Mitchell LG, McGarrity GJ. Gene therapy progress and prospects: reprograming gene expression by trans-splicing. Gene Ther 2005;12:1477–85.
18. Bhakdi S, Bayley H, Valeva A, Walev I, Walker B, Kehoe M, et al. Staphylococcal alpha-toxin, streptolysin-O, and Escherichia coli hemolysin: prototypes of pore-forming bacterial cytolysins. Arch Microbiol 1996;165:73–9.
19. Chakraborti S, Mandal M, Das S, Mandal A, Chakraborti T. Regulation of matrix metalloproteinases: an overview. Mol Cell Biochem 2003;253:269–85.
20. Rodriguez-Martin T, Garcia-Blanco MA, Mansfield SG, Grover AC, Hutton M, Yu Q, et al. Reprogramming of tau alternative splicing by spliceosome-mediated RNA trans-splicing: implications for tauopathies. Proc Natl Acad Sci U S A 2005;102:15659–64.
21. Zayed H, Xia L, Yerich A, Yant SR, Kay MA, Puttaraju M, et al. Correction of DNA protein kinase deficiency by spliceosome-mediated RNA trans-splicing and sleeping beauty transposon delivery. Mol Ther 2007;15:1273–9.
22. Liu X, Jiang Q, Mansfield SG, Puttaraju M, Zhang Y, Zhou W, et al. Partial correction of endogenous DeltaF508 CFTR in human cystic fibrosis airway epithelia by spliceosome-mediated RNA trans-splicing. Nat Biotechnol 2002;20:47–52.
23. Thomas SM, Grandis JR. The current state of head and neck cancer gene therapy. Hum Gene Ther 2009;20:1565–75.
24. Chao H, Mansfield SG, Bartel RC, Hiriyanna S, Mitchell LG, Garcia-Blanco MA, et al. Phenotype correction of hemophilia A mice by spliceosome-mediated RNA trans-splicing. Nat Med 2003;9:1015–9.
25. Puttaraju M, DiPasquale J, Baker CC, Mitchell LG, Garcia-Blanco MA. Messenger RNA repair and restoration of protein function by spliceosome-mediated RNA trans-splicing. Mol Ther 2001;4:105–14.
26. Yamaizumi M, Mekada E, Uchida T, Okada Y. One molecule of diphtheria toxin fragment A introduced into a cell can kill the cell. Cell 1978;15:245–50.
27. Wanebo HJ, Blackinton D, Kouttab N, Mehta S. Contribution of serum inhibitory factors and immune cellular defects to the depressed cell-mediated immunity in patients with head and neck cancer. Am J Surg 1993;166:389–94.
28. Whiteside TL. Immunobiology of head and neck cancer. Cancer Metastasis Rev 2005;24:95–105.
29. Matzinger P. An innate sense of danger. Semin Immunol 1998; 10:399–415.
30. Hobohm U, Stanford JL, Grange JM. Pathogen-associated molecular pattern in cancer immunotherapy. Crit Rev Immunol 2008;28:95–107.